Above-Threshold Ionization in the Long-Wavelength Limit

P. B. Corkum, N. H. Burnett, and F. Brunel

Division of Physics, National Research Council of Canada, Ottawa, Ontario, Canada K1A 0R6

In the long-wavelength limit, above-threshold ionization (ATI) is primarily the result of the interaction of a newly freed electron with the laser field. Classical physics requires that linearly and circularly polarized light produce very different ATI spectra. Measurements performed using both linearly and circularly polarized, picosecond, 10-μm pulses confirm these conclusions.

PACS numbers: 32.80.−t

Above-threshold ionization (ATI) provides a new controllable heating mechanism for plasmas. It will be particularly important at low densities where other heating mechanisms are ineffective.

This paper provides new understanding of above-threshold ionization[1] with ultrashort pulses. It also provides the first direct evidence of tunnel ionization at optical frequencies.[2] We show that in the quasiclassical limit (photon energy less than ionization potential less than ponderomotive energy), an electron acquires its energy in a two-step process: First, the electron is removed (tunnels) from the primary influence of the atom, thereby absorbing the ionization potential, and then it interacts with the laser field. The second step, which can be treated classically, also consists of two parts. There is the ponderomotive (i.e., quiver) component of the interaction[3] and also a drift component. For linearly polarized light, the magnitude of the drift component is determined by the exact phase of the electric field at which the electron is freed. The drift energy has never been explicitly considered and is the main subject of this paper.

For ultrashort pulses the ponderomotive energy is returned to the wave[4] and it does not contribute to ATI; however, the drift motion remains. Thus the classical theory gives a different perspective for understanding the ATI in the high-intensity–long-wavelength limit. Furthermore, the difference that we find in the drift energy between linearly and circularly polarized light gives a new point of view on why higher-energy electrons have been found for circularly polarized light in previous experiments.[5]

Consider an electron released at time t' from rest into a strong laser field. The electron will experience a force which, in the nonrelativistic limit, is proportional to the electric field $\mathbf{E} = E_0\cos(\omega t)\mathbf{e}_x + \alpha E_0\sin(\omega t)\mathbf{e}_y$ where $\alpha \leq 1$ allows for arbitrary polarization.

The electron motion in the field of the laser is given by

$$v_x = v_0\sin(\omega t) + v_{0x}, \quad v_y = -(\alpha v_0)\cos(\omega t) + v_{0y}, \qquad (1)$$

where $v_0 = qE_0/m\omega$ and v_{0x} and v_{0y} can be evaluated from the initial condition that $v_x(t') = v_y(t') = 0$ to be $v_{0x} = -v_0\sin(\omega t')$ and $v_{0y} = \alpha v_0\cos(\omega t')$.

The probability of ionization as a function of time can be calculated in the quasistatic limit ($E_i < U$) using dc tunneling theory[6]:

$$w(t) = 4\omega_0 \left[\frac{E_i}{E_h}\right]^{5/2} \frac{E_a}{E(t)} \exp\left[-\frac{2}{3}\left[\frac{E_i}{E_h}\right]^{3/2}\frac{E_a}{E(t)}\right], \qquad (2)$$

where $\omega_0 = me^4/\hbar^3$ is the atomic frequency unit, E_h and E_i are the ionization potentials of hydrogen and the atom in question, $U = (1+\alpha^2)q^2E^2/4m\omega^2$ is the ponderomotive potential, and $E_a = m^2e^5/\hbar^4$ is the atomic unit of the electric field. Applying Eq. (2) for a hydrogenlike ion with $E_i = 12.1$ eV (xenon), the electron distribution shown in Fig. 1 (solid curve) is obtained for a 10-μm linearly polarized plane wave ($\alpha = 0$) with intensity $I = 10^{14}\exp[-(t/\tau)^2]$ W/cm^2 and $\tau = 1.5$ psec. For linearly polarized light the calculated ionization rate was 10^{12} sec^{-1} at an intensity of 6×10^{13} W/cm^2.

For circularly polarized light ($\alpha = 1$), we can always
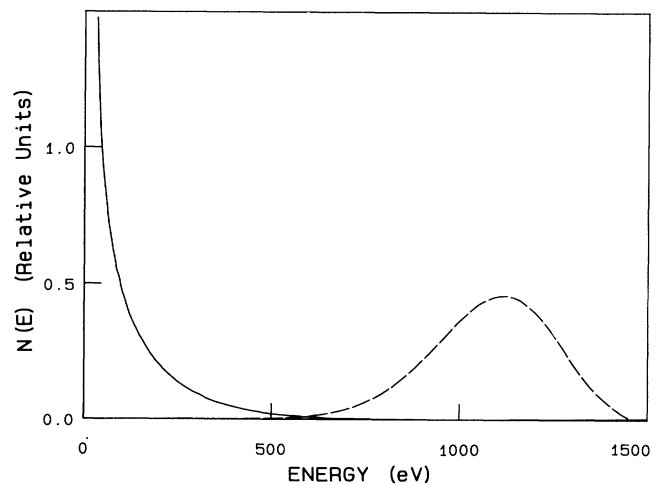
FIG. 1. Electron energy distribution calculated using the classical theory of above-threshold ionization for a hydrogenlike ion with an ionization potential of 12.1 eV. Linearly polarized (solid curve, peak intensity of 10^{14} W/cm^2) and circularly polarized (dashed curve, peak intensity of 2×10^{14} W/cm^2) 10-μm radiation and 2.5-psec FWHM Gaussian pulses were assumed.

orient the coordinate system so that $t'=0$. The initial conditions then give a drift velocity of $v_{0x}=0$ and $v_{0y}=v_0$. That is, the electron drifts in a direction perpendicular to the field in which it was released (ionized). Using dc tunneling rates ($E_i=12.1$ eV), the electron distribution shown in Fig. 1 (dashed curve) is obtained for a 10-μm plane-wave pulse given by $I=(2\times10^{14})\exp[-(t/\tau)^2]$ W/cm^2 where $\tau=1.5$ psec. For circularly polarized light the calculated ionization rate was 10^{12} sec^{-1} at an intensity of 9.5×10^{13} W/cm^2.

Whereas the width of the distribution for linearly polarized light is determined by the phase angle at which the electron is produced, the width for circularly polarized light is characteristic of the pulse envelope. Under experimental conditions the volume associated with a particular intensity increases as the intensity decreases. Thus, most electrons are produced near the peak power portion of the temporal profile. The distribution would then be slightly narrower than that shown in Fig. 1.

To confirm these predictions, an experiment was performed using a picosecond, 9.3-μm pulse produced in a laser system described elsewhere.[7] For the present experiment the maximum pulse energy was 60 mJ. The coherent structure of the pulse is such that 65% of the energy is in a 2.5-psec FWHM ($\tau=1.5$ psec) pulse.[8] Most of the remainder appears 25 psec later in a second 2.5-psec pulse. Thus the peak laser power was as high as 2.5×10^{10} W.

The laser was designed to produce linearly polarized light. The plane of polarization was changed by adding an additional reflecting surface along the path followed by the beam as it was transported from the laser to the target chamber. Circularly polarized light was produced by passing the beam through a Fresnel rhomb. The beam was focused into a target chamber with either a 25-cm (linearly polarized) or a 12.5-cm (circularly polarized) lens to a beam waist of 170 or 85 μm full width at half maximum. The focal-spot intensities were 8×10^{13} and 3×10^{14} W/cm^2, respectively.

The target chamber could be pumped to a background pressure of 10^{-9} Torr. A xenon pressure of $\sim10^{-6}$ Torr was used for all measurements. The beam was focused between parallel electrodes that could be biased so as to extract either electrons or ions which were measured by an electron multiplier. Time of flight was used to establish the ion species. Only Xe^{+1} was present in the measurements described herein.

The electron energy spectrum was determined by collecting those electrons with sufficient energy to pass through a grid biased with a retardation potential. Any detected electron possessed sufficient drift energy in the direction of the electron multiplier to overcome the retardation potential minus that portion of the extraction potential seen by the electron. The detected signal is $S(E_0)=\int_{E_0}^{\infty}n(E)dE$, where $n(E)$ is the number of electrons with drift energy E.

For linearly polarized light, an extraction field was ap-
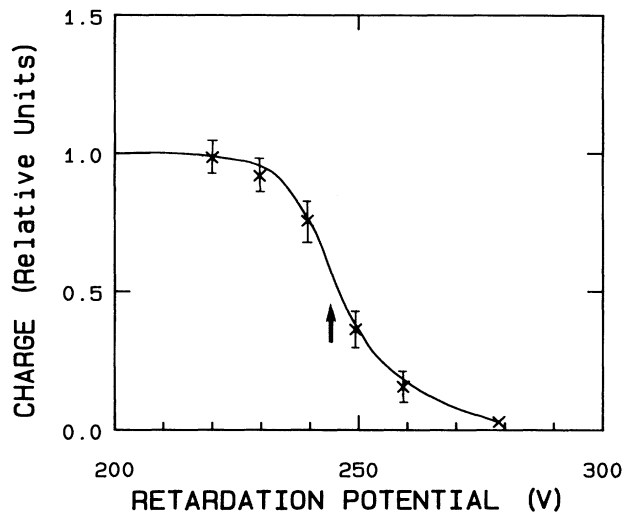
FIG. 2. Relative number of ATI electrons with drift energy in excess of the retardation potential plotted as a function of the retardation potential. A 2.5-psec, 9.3-μm laser pulse was used to ionize 10^{-6} Torr of xenon. The direction of observation was perpendicular to the electric vector of the laser field and the direction of propagation. The laser focus was at a potential of 240 V as noted by the arrow.

plied to ensure that all electrons were collected. Figure 2 is a graph of the electron energy observed with the electric field of the 9.3-μm radiation perpendicular to the direction of the extraction and retardation fields. Classically the drift energy in this direction should be zero. This fact is used to calibrate the extraction potential as seen by the electrons at 240 V (the potential difference across the electrodes was 400 V, the focal position was reproducible and consistent with an extraction potential of 240 V). If 240 eV is subtracted from the electron energy, we obtain a typical energy in the direction perpendicular to the laser field of < 10 eV. Considering the electrical noise in the vicinity of the measurement, the mechanical stability of the apparatus, and the accuracy with which we know that our beam is linearly polarized, this is probably the resolution limit of the experiment.

The distribution of electron energies measured with the electric field of the ionizing radiation pointing in the direction of the extraction and retardation potentials is shown in Fig. 3. The 240-V extraction field has been subtracted from the measured electron energy. It is clear from a comparison of Figs. 2 and 3 that the electrons drift primarily along the direction of the laser field with an average energy of approximately 50 eV.

For linearly polarized light, ionization occurs at approximately 5×10^{13} W/cm^2. Thus for our 2.5-psec pulse, the electron is left with < 10% of the ponderomotive potential after the laser pulse has passed. Figure 3 (solid curve) shows the calculated value of $S(E_0)$ for 9.3-μm light. It is important to know whether 50 eV is an accurate estimate of the drift energy. The velocity of
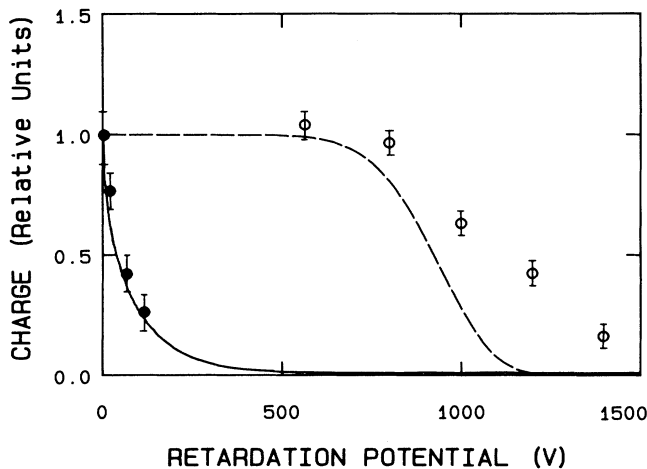
FIG. 3. Relative number of ATI electrons with drift energy in excess of the retardation potential plotted as a function of the retardation potential. Electron energy measured (solid circles) and calculated (solid curve) in the direction of the laser electric field vector. The 240-V extraction potential was subtracted from the experimental data. Also shown are experimental data (open circles) and calculations (dashed curve) obtained with circularly polarized 9.3-μm light.

a 50-eV electron is approximately $0.01c$. Such an electron will drift less than one wavelength during the fall time (τ) of the laser pulse. Since the laser barely exceeded the threshold intensity, ionization occurs primarily on axis. Thus, the electrons will gain negligible energy from the ponderomotive force. We expect, and observe in Fig. 3, good agreement between the quasistatic model and the experimental results.

Figure 3 also shows the electron energy distribution obtained with circularly polarized light. A typical electron energy is 1200 eV (velocity=20 μm/psec). Thus, in contrast to the linearly polarized case, the ponderomotive force will make a significant contribution to the measured electron energy spectrum.

It should be emphasized that the ponderomotive force is insufficient to account for the distribution on its own. To see this, consider the extreme case of the electrons produced at the beam waist and at the radius of maximum ponderomotive force. Since our (calculated and experimental) threshold intensity for circularly polarized light is approximately 10^{14} W/cm^2, these electrons will be produced during the rising portion of the pulse. If their initial drift velocity is negligible, they can gain only 600 eV due to ponderomotive acceleration. This overes-

timates the contribution of the ponderomotive force for two reasons. (1) Most electrons in a Gaussian focus are produced at the time of peak power. In the absence of an initial drift energy, these electrons can gain a maximum energy of only 250 eV. (2) Most electrons are produced at radii and a focal position at which the ponderomotive force is less than the maximum. Without a large initial drift energy these electrons can gain even less energy.

In Fig. 3, the dashed curve shows the calculated value of $S(E_0)$ from the plane-wave classical mode. Considering random distribution of ionization sites and the random direction of the electrons, the motion in ponderomotive potential will broaden the electron spectrum and add a significant fraction of the ponderomotive energy to the most favorably directed and positioned electrons. The ponderomotive contribution accounts for much of the differences between experiment and the predictions of the classical model (Fig. 3, dashed curve).

The approach that we have taken is very reminiscent of Keldysh style theories.[9] Keldysh theories dress the outgoing electron for the effects of the optical field. The ionization rate is then determined by a first-order perturbation calculation of the transition probability from the ground state to the dressed free state of the electron. In our classical theory of ATI we have dressed the electron classically rather than quantum mechanically for the effects of the laser field. In fact, assuming that tunnel ionization determines the ionization probability as a function of the electric field, it can be shown that the classical model with zero initial velocity gives electron distributions that are almost indistinguishable from those implicit in Keldysh's work[9] and are similar to the predictions of Reiss[10] for linearly polarized light.

For circularly polarized light, the drift energy gained by the electron during ionization is also consistent with the quantum-mechanical picture of Reiss.[10] From Eq. (32) of Ref. 10, the ionization rate per unit solid angle is given by

$$\frac{dW}{d\Omega} = \frac{(2m^3\omega^5)^{1/2}}{(2\pi)^2}\sum_n (n-z)^2(n-z-\epsilon_B)^{1/2}$$

$$\times |\hat{\phi}_i(\mathbf{p})| J_n^2(z^{1/2}\gamma), \quad (3)$$

where $\gamma=2(n-z-\epsilon_B)^{1/2}\sin\theta$. θ is defined with respect to the axis of propagation, $\epsilon_B=E_i/\hbar\omega$, and $z=U/\hbar\omega$. For other symbols, see Ref. 10.

In the low-frequency limit, the argument $z^{1/2}\gamma$ of the Bessel function in Eq. (3) becomes very large and $J_n^2(z^{1/2}\gamma)$ becomes highly peaked around $n=2z$ and can be written as

$$J_{2z+\delta n}^2 = \frac{1}{2\pi(4z\epsilon_B)^{1/2}}\exp\left[-\frac{4\epsilon_B^{3/2}}{3z^{1/2}} - 2\epsilon_B^{1/2}z^{1/2}\delta\theta^2 - \frac{\epsilon_B^{1/2}\delta n^2}{2z^{3/2}}\right], \quad (4)$$

where $\delta n = n - 2z$ and $\delta\theta = (\pi/2) - \theta$. This expression is valid providing $\epsilon_B^{3/2}/z^{1/2}$ is large, corresponding to the same limit of validity as Eq. (2).

One can see from Eq. (4) that the electron distribution is highly peaked around $n=2z$ (i.e., around an electron energy of twice the ponderomotive energy). Since the system is in a steady-state electromagnetic field, the drift energy is obtained by subtracting the ponderomotive energy. The drift energy, therefore, peaks at a value corresponding to the classical value of v_{0y} in Eq. (1). The distribution is also highly peaked around $\theta=\pi/2$ as prescribed by the classical model.

From the width of the distribution in $\delta\theta$ or δn, an uncertainty $\delta\epsilon$ can be found in the initial kinetic energy of the electron after ionization. Thus we can check if our assumption that the initial velocity of the electron is zero at $t=t'$ is consistent with Keldysh-Reiss theory. Since $\delta\theta=\delta v_\perp/v_{0y}$ and also $\delta n/z=2\delta v_\parallel/v_{0y}$ [$\delta v_\perp$ and $\delta v_\parallel$ are the uncertainties in the initial velocity in the direction perpendicular and parallel to the drift v_{0y} and $\delta\epsilon=m(\delta v_\perp)^2/2=m(\delta v_\parallel)^2/2$] then we obtain $\delta\epsilon/U=\langle\delta\theta^2\rangle=\langle\delta n^2\rangle/4z^2=(2\epsilon_B^{1/2}z^{1/2})^{-1}$ or $\delta\epsilon=\hbar\omega z^{1/2}/2\epsilon_B^{1/2}$. This value of $\delta\epsilon$ is consistent with an uncertainty of $\delta\epsilon=h/\Delta t$, where Δt is the tunneling time given by $\Delta t=E_i^{1/2}(m^{1/2}\omega/eE_0)/\omega$ as discussed in the introduction in Ref. 9. For the parameters of this experiment the uncertainty in the initial energy is $\delta\epsilon=0.4$ eV. Numerical calculations using Reiss's theory for the angular spread of the electrons produced by linearly polarized light are consistent with the same $\delta\epsilon$.

Aside from its intrinsic interest, ATI will be important in a general sense for plasma physics. By varying the polarization and wavelength of the ultrashort ionizing laser pulse, the electron temperature of an underdense plasma can be chosen. For near uv laser radiation, we estimate that plasmas with electron temperatures of about 10% of the ionization potential can be generated for ionization potentials up to 100 eV. On the other extreme, consider a helium plasma ionized by circularly polarized, picosecond, 10-μm radiation. The calculated electron energy is 10 keV. If the second electron is removed from the helium by the laser field, the energy of this additional electron would be >100 keV (the classical theory of ATI can be readily generalized to the relativistic case). To form a thermalized plasma the electrons must be confined electrostatically and electron-electron scattering is required.

Note added.—Some aspects of the classical model have been recently discussed in the context of microwave ionization experiments by Gallagher.[11]

[1]P. Agostini, F. Fabre, G. Mainfray, G. Petite, and N. K. Rahman, Phys. Rev. Lett. **42**, 1127 (1979).

[2]F. Yergeau, S. L. Chin, and P. Lavigne, J. Phys. B **20**, 723 (1987).

[3]T. J. McIlrath, P. H. Bucksbaum, R. R. Freeman, and M. Bashkansky, Phys. Rev. A **35**, 4611 (1987).

[4]R. R. Freeman, P. H. Bucksbaum, H. Milchberg, S. Darack, D. Shumacher, and M. E. Geusic, Phys. Rev. Lett. **59**, 1092 (1987).

[5]P. H. Bucksbaum, M. Bashkansky, R. R. Freeman, T. J. McIlrath, and L. F. DiMauro, Phys. Rev. Lett. **56**, 2590 (1986).

[6]L. D. Landau and E. M. Lifshitz, *Quantum Mechanics* (Pergamon, New York, 1965), 2nd ed., p. 276.

[7]P. B. Corkum and C. Rolland, Proc. SPIE **664**, 212 (1986).

[8]P. B. Corkum, IEEE J. Quantum Electron. **21**, 216 (1985).

[9]L. V. Keldysh, Zh. Eksp. Teor. Phys. **47**, 1945 (1964) [Sov. Phys. JETP **20**, 1307 (1965).]

[10]H. R. Reiss, Phys. Rev. A **22**, 1786 (1980).

[11]T. F. Gallagher, Phys. Rev. Lett. **61**, 2304 (1988).